Int J Infrared Milli Waves (2008) 29:385–395
DOI 10.1007/s10762-008-9334-0

Infrared Small Target Detection Using PPCA

Yuan Cao · RuiMing Liu · Jie Yang

Received: 29 September 2007 / Accepted: 24 January 2008 /
Published online: 19 February 2008

Abstract Probabilistic PCA (PPCA) is an extension of PCA which reformulated PCA in a probabilistic framework. In this paper we propose a infrared small target detection algorithm using PPCA analogous to the face detection scheme using PCA, or known as "eigenface". By computing the parameters of PPCA, we map the input vector from the image onto a subspace. After reconstructing the vector, the distance between the original vector and the reconstructed one will indicate the possibility of the input being a target. Experimental results show the effectiveness of this algorithm compared with other methods.

Keywords Target detection · Infrared image · PPCA

1 Introduction

Detecting small targets in infrared images has been a difficult task because of the small scale of the target, the low signal-to-background ratio and the lack of target color or clear shape information. Lots of image processing techniques have been used in small target detection, for example Soni *et al*. proposed a detection algorithm based on adaptive TDLMS(two dimensional LMS) filter [10]; Boccignone *et al*. proposed an algorithm based on wavelet transform [4] and Sadjadi proposed an algorithm using probability functions of the subband of the wavelet decomposition of an image [5]; Kwon *et al*. proposed an algorithm by using kernel spectral matched filter [6]; Leung *et al*. proposed an algorithm using recursive non-linear background prediction [7].

The infrared small target detection problem can also be regarded as a two-class pattern recognition problem: targets can be detected and captured if we are able to separate the target class and the background class effectively. Mahalanobis *et al*. proposed a target detection algorithm using the Fukunaga-Koontz transform (FKT) which is an effective two class pattern recognition method [11]; Dwan *et al*. applied neural network in the target

Y. Cao (✉) · R. M. Liu · J. Yang
Institute of Image Processing and Pattern Recognition, Shanghai Jiao Tong University,
No. 800 Dongchuan Road, Shanghai 200240, People's Republic of China
e-mail: cao_yuan@sjtu.edu.cn

detection scheme [13]; Liu *et al*. proposed a target detection algorithm based on nonlinear PCA neural network [12]; Chan *et al*. proposed an algorithm by combining neural-network-based PCA and a backpropagation learning algorithm [8].

PCA is one of the most popular methods in removing redundancies in high dimensional data by finding a lower dimensional linear subspace that best captures the data characteristics. However, conventional PCA does not correspond to a probabilistic density. Tipping and Bishop [1, 2] reformulated PCA in a probabilistic framework, known as probabilistic PCA (PPCA). As an extension of PCA, PPCA keeps the merits of conventional PCA and can also model the Gaussian density of the high dimensional observation space. In conventional PCA, the information outside the subspace is simply discarded, however PPCA estimates this information by regarding it as Gaussian noise. PPCA defined a proper probabilistic model, this model can be easily extended to a mixture model, and the parameters of this algorithm can be obtained by using an EM algorithm.

By applying PCA, Turk and Pentland proposed a well-known face recognition algorithm using "eigenface" [9]. We would like to perform target detection by referring to this methodology, but replacing PCA with PPCA as a data dimension reduction algorithm, in view of utilizing the feature of PPCA and its advantage over PCA. This paper is organized as the following: Section 2 briefly introduces the theory of PPCA; Section 3 proposed the target detection algorithm using PPCA; experimental results and analysis are given in Sections 4 and 5 makes the conclusion.

2 Probabilistic PCA

PPCA essentially augments the linear mapping from PCA to the observed data space by assuming that the observed data be corrupted by isotropic Gaussian noise, and the PCA coefficients to follow an isotropic Gaussian distribution in the embedding subspace. In the case where the observation noise variance goes to zero, the standard PCA is recovered.

PPCA is formulated from a Gaussian latent variable model. A latent variable model tries to relate a d dimensional data x to a corresponding q dimensional latent variable z, where $q<d$. In standard factor analysis, the relationship between x and z is linear:

$$x = Wz + \mu + \varepsilon \tag{1}$$

where the latent variables $z \sim N(0,\ I)$ and have a unit isotropic Gaussian, $\mu = \frac{1}{N}\sum_{i=1}^{N} x_i$ is sample data mean, the noise model Gaussian $\varepsilon \sim N(0, \psi)$ with diagonal covariance matrix ψ and z is dependent of ε. From the linear relationship variable x also has Gaussian distribution $x \sim N(\mu,\ WW^T + \psi)$.

The probabilistic model of PPCA is given in Tipping and Bishop [1] and [2]. Assume noise $\varepsilon \sim N(0,\ \sigma^2 I)$ and the prior distribution of the latent variable z is

$$p(z) = \left(2\pi\sigma^2\right)^{-\frac{q}{2}} \exp\left\{-\frac{1}{2}z^T z\right\} \tag{2}$$

According to Eq. 1, the observed data x will have the distribution of

$$p(x|z) = \left(2\pi\sigma^2\right)^{-\frac{d}{2}} \exp\left\{-\frac{\|x - Wz - \mu\|^2}{2\sigma^2}\right\} \tag{3}$$

The marginal distribution of the observed data x is obtained by integrating out the latent variable as the following:

$$p(x) = \int p(x|z)p(z)dz = (2\pi)^{-\frac{d}{2}}\left|\sum\right|^{-\frac{1}{2}} \exp\left\{-\frac{1}{2}(x-\mu)^T\sum^{-1}(x-\mu)\right\} \tag{4}$$

where the covariance is specified by $\sum=WW^T+\sigma^2 I$ and this implies $x\sim N(\mu, \sigma)$.

The posterior distribution of the latent variable z can be calculated using the Bayesian formula as:

$$p(z|x) = (2\pi)^{-\frac{q}{2}}\left|\sigma^{-2}C\right|^{\frac{1}{2}} \exp\left[-\frac{1}{2}\left\{z - C^{-1}W^T(x-\mu)\right\}^T \times\left(\sigma^{-2}C\right)\left\{z - C^{-1}W^T(x-\mu)\right\}\right] \tag{5}$$

where $C=W^TW+\sigma^2T$. Therefore the distribution can be used to predict z for a given x.

The goal is to determine W and σ such that the data x_i if drawn from x are most likely. Parameters W and σ can be obtained by using expectation-maximization algorithm (EM) which is an iterative method. The log-likelihood of (2)(3) is defined as

$$L = \sum_{i=1}^{N}\ln\{p(x_i,z_i)\} = \sum_{i=1}^{N}\ln\left[\left(2\pi\sigma^2\right)^{-\frac{d}{2}}\exp\left\{-\frac{\|x_i - Wz_i - \mu\|^2}{2\sigma^2}\right\} \times(2\pi)^{-\frac{q}{2}}\exp\left\{-\frac{z_i^Tz_i}{2}\right\}\right] \tag{6}$$

In the E-step, the expectation of L is taken as

$$E\{L\} = -\sum_{i=1}^{N}\left[\frac{d}{2}\ln\sigma^2 + \frac{1}{2}tr\left(E\left\{z_iz_i^T\right\}\right) + \frac{\|x_i-\mu\|^2}{2\sigma^2} - \frac{1}{\sigma^2}E\{z_i\}^TW^T(x_i-\mu) + \frac{1}{2\sigma^2}tr\left(W^TWE\left\{z_iz_i^T\right\}\right)\right] \tag{7}$$

where $E\{z_i\}=C^{-1}W^T(x_i-\mu)$ and $E\{z_iz_i{}^T\}=\sigma^2C^{-1}+E\{z_i\}E\{z_i\}^T$.

In the M-step, $E\{L\}$ is maximized with respect to W and σ^2 by differentiating (7) and setting the derivatives to zero. The new parameter estimates are

$$W = \left[\sum_{i=1}^{N}(x_i-\mu)E\{z_i\}^T\right]\left[\sum_{i=1}^{N}E\left\{z_iz_i^T\right\}\right]^{-1} \tag{8}$$

$$\sigma^2 = \frac{1}{Nd}\sum_{i=1}^{N}\left[\|x_i-\mu\|^2 - 2E\{z_i\}^TW(x_i-\mu) + tr\left(E\left\{z_iz_i^T\right\}W^TW\right)\right] \tag{9}$$

By replacing $C=W^TW+\sigma^2I$ we get

$$\overline{W} = SW\left(\sigma^2 I + M^{-1}W^T SW\right)^{-1} \tag{10}$$

$$\sigma^2 = \frac{1}{d}tr\left(S - SWM^{-1}\overline{W}^T\right) \tag{11}$$

where $S = \frac{1}{N}\sum_i^N (x_i-\mu)(x_i-\mu)^T$ is the covariance matrix of the samples. Now it can be seen that W and σ^2 can be computed iteratively until Eqs. 10 and 11 converge.

In Tipping and Bishop [2], it is concluded that the reduced-dimensionality of a data point x_i can be computed as $t_i=W^T(x_i-\mu)$, and the data point can be optimally reconstructed using

$$\widehat{x_i} = W\left(W^TW\right)^{-1}t_i + \mu. \tag{12}$$

3 Detecting small target using PPCA

The PPCA algorithm introduced above can be used to perform small target detection in infrared images. The idea is enlightened by the face detection method using PCA introduced by Turk and Pentland [9, 10]. In this scheme, principle component analysis of a training set of face images is performed to generate the eigenpictures (called eigenface) which span a subspace (called the face space) of the image space. Images of faces are projected onto this subspace and clustered. Since face images do not change radically when projected onto the face space while the projection of non-face images will appear quite different, the detection of face can be done by measuring the distance from the face space.

By referring to the face detection scheme using PCA, we first replace the dimension reduction algorithm PCA with PPCA, and then determine the steps for target detection algorithm, as the following:

1. Given N training target images of size $m\times m$, reshape each image into a vector Γ_i, and compute the mean vector $\overline{\Gamma}$. Compute the zero-mean data $\Phi_i = \Gamma_i - \overline{\Gamma}$, and then combine them into a matrix $C=[\Phi_1, \Phi_2 \cdots \Phi_N]$.
2. Initialize parameters W_0 and ${\sigma_0}^2$, compute iteratively using the EM algorithm given in Eqs. 10 and 11 until the parameters converge, so that parameters W and σ^2 can be determined.
3. Scan the image to be detected block after block, the size of each block being $m\times m$. Reshape the block matrix into a vector X of size $m^2\times 1$ and centralize the data using $X' = X - \overline{\Gamma}$.
4. Compute the weights in the subspace for each new block: $\Omega=W^TX'$.
5. Reconstruct the block vector by computing $\widehat{X} = W(W^TW)^{-1}\Omega$.
6. Compute the Euclidean distance between X' and $\widehat{X}$: $d = \left\|X' - \widehat{X}\right\|$. A small d indicates a target block while a large d indicates a background clutter block. Define $S(X) = \exp\left(-\left\|X' - \widehat{X}\right\|^2\right)$ as a saliency measure function, and a large $S(X)$ will correspond to the position of targets.

For the algorithm above, how to generate the training samples of small targets is critical and can much influence the detection results. In Liu *et al.* [12], it is introduced that the training sample of small targets can be generated by using the Gaussian intensity function, which is

$$I(x,y) = I_{\max} \exp\left(-\frac{1}{2}\left[\frac{(x-x_0)^2}{\sigma_x^2} + \frac{(y-y_0)^2}{\sigma_y^2}\right]\right) \tag{13}$$

The pixel spread characteristics of simulated targets are defined by the maximum intensity $I_{\max}$, horizontal spread parameter σ_x and vertical spread parameter σ_y. (x_0, y_0) is the center location of the target with the intensity value $I_{\max}$. By choosing different $I_{\max}$, σ_x and σ_y, different simulated small targets can be generated and used as training samples.

Of course, the training samples of small targets can also be obtained by cropping blocks from real infrared images containing targets, however we prefer to use the method to generate training targets introduced above for the following reasons: first it is not easy to decide the exact position of small targets in images before they are detected; secondly, in real infrared images the target areas could often be contaminated by noises, therefore they may fail to present the exact property of small targets; what is more, it would be a real laborious work to crop hundreds of small blocks containing targets from a number of real images if we need that many training samples.

4 Experimental results

In our experiments, we choose the size of the training targets samples as 11×11, which means the dimension of x in (1) will be d=121, and we choose q=5. 121 training target

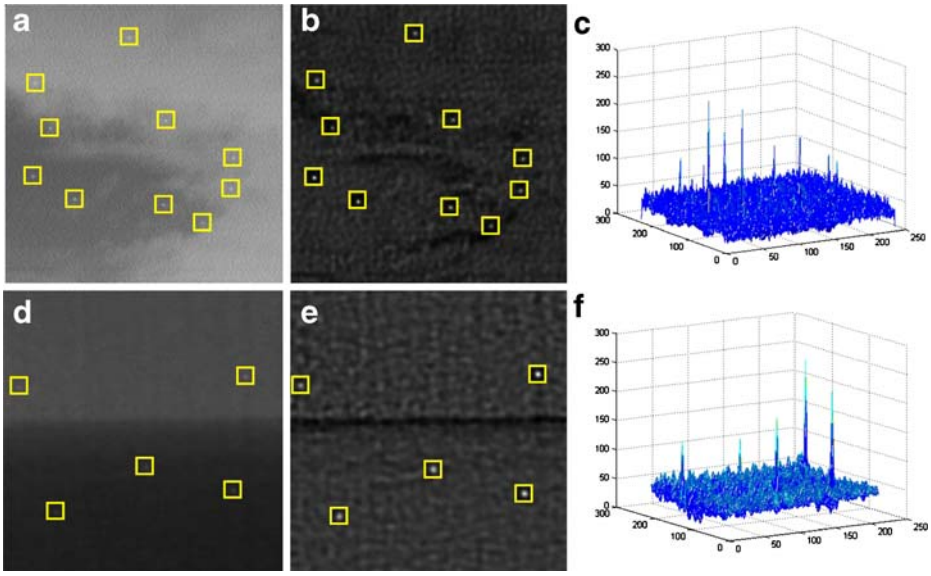

Fig. 1 Infrared images containing multiple small targets and their detection results. (**a**, **d**) original image (**b**, **e**) output image after detection (**c**, **f**) intensity plot of the output images.

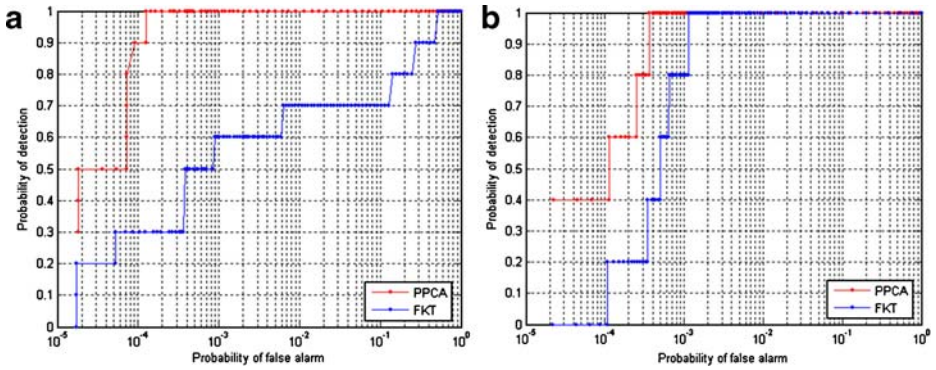

Fig. 2 ROC curves of the output images after detection in Fig. 1. **a** ROC curve for Fig. 1(b); **b** ROC curve for Fig. 1(e).

samples are generated using (13) randomly. First we choose two infrared test images which contain multiple targets in our experiments as is shown in the first column in Fig. 1, in which the first image contains ten targets and the second one contains five targets. The targets are very small, weak and dim thus are pretty hard to detect. Second column in Fig. 1 shows the detection output using the algorithm introduced in Section 3, and the third column corresponds to the intensity plot of the second column after detection. It can be seen that using the proposed algorithm, all the targets in the test images are very clearly detected and made easy to identify.

The receiver operating characteristic (ROC) curve is also shown to evaluate the performance of the proposed algorithm. We compare the proposed algorithm with another effective target detection algorithm using Fukunaga-Koontz transform [11] in the ROC curve in Fig. 2, where (a) corresponding to the detection result of Fig. 1 (a) and (b) corresponding to the detection result of Fig. 1 (d). The ROC curves are constructed by varying the detection threshold (ROC operating point). It can be seen from the curve that when PPCA and FKT has the same false alarm probability, the detection probability of PPCA is much higher than FKT. This means that after detection using PPCA, targets are more distinguishable from background than using FTK. Therefore, PPCA has a much better performance than FKT in target detection.

In order to show the robustness of the proposed algorithm, in Fig. 3 another 6 infrared images containing small targets are used to for experiments. Figure (a) and (d) correspond to images with sky background, (g) and (j) correspond to images with sea background, (m) and (p) correspond to the images with earth background. Second column of Fig. 3 show the output images after detection and the third column show the corresponding intensity plot. It can be seen from Fig. 3 that by using our proposed algorithm, the backgrounds in test images are all successfully suppressed and the targets are clearly detected.

To further validate the performance of the proposed algorithm, we compare PPCA with several other small target detection methods such as max-median (M-Med) filter, max-mean (M-Mean) filter [9], two-dimensional LMS (TDLMS) filter [10] and FKT by numerical values. The detectability of the small target depends on the signal to background ratio in its

Fig. 3 Infrared images for experiments. First column: original images. Second column: output images after detection. Third column: intensity plot of output images.

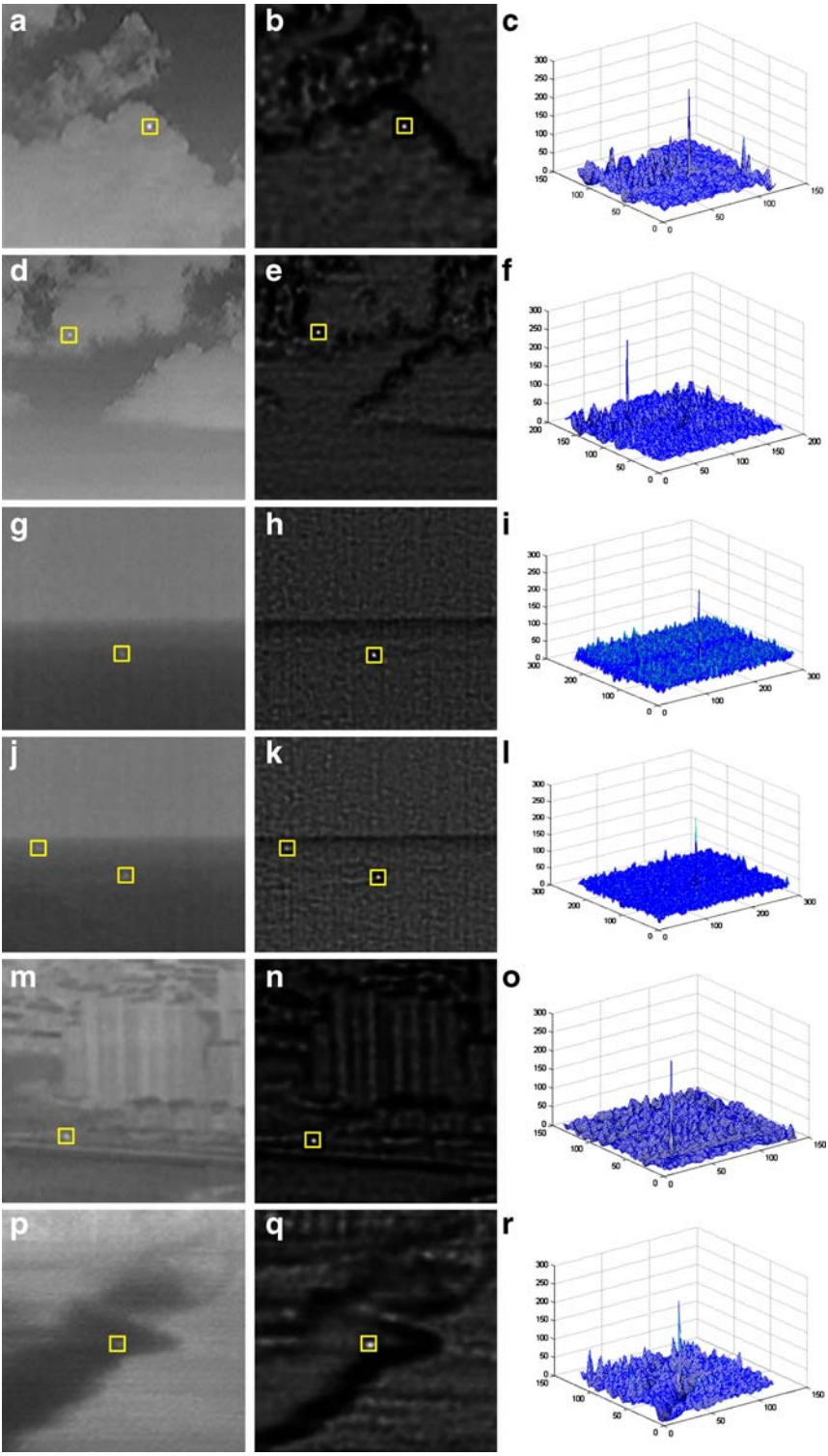
a
b
c
d
e
f
g
h
i
j
k
l
m
n
o
p
q
r

Table 1 Comparison of several small target detection algorithms for Fig. 1.

	Target	*LSBR*					*LSBRG*				
		M-Med	M-Mean	TDLMS	FKT	PPCA	M-Med	M-Mean	TDLMS	FKT	PPCA
Fig. 1(a)	1	0.868	−1.522	1.651	10.378	24.501	−8.841	−11.232	−8.058	0.6685	14.791
	2	7.423	5.589	5.272	3.665	20.214	−0.106	−1.940	−2.256	−3.864	12.684
	3	8.773	7.295	5.934	3.698	17.298	3.929	2.451	1.091	−1.145	12.454
	4	3.471	2.501	0.610	−3.234	16.294	−0.308	−1.278	−3.169	−7.014	12.514
	5	0.290	−0.223	−3.157	−5.251	15.959	−2.117	−2.631	−5.565	−7.659	13.551
	6	2.025	3.137	−0.446	6.377	15.025	−2.422	−1.309	−4.893	1.930	10.578
	7	0.821	−1.239	−1.302	0.201	13.095	0.374	−1.686	−1.749	−0.246	12.648
	8	3.389	1.498	−4.252	−4.376	16.278	1.039	−0.851	−6.602	−6.726	13.929
	9	0.157	−0.460	0.981	0.649	14.723	−3.238	−3.856	−2.414	−2.746	11.327
	10	2.973	3.009	−0.038	4.928	15.657	1.653	1.689	−1.359	3.607	14.337
Fig. 1(d)	1	15.823	13.914	9.630	1.900	23.256	−0.4271	−2.336	−6.620	−14.351	7.005
	2	19.795	15.417	14.442	7.916	21.549	3.9664	−0.411	−1.387	−7.912	5.720
	3	10.526	7.859	6.360	7.616	18.573	−3.3532	−6.020	−7.519	−6.263	4.693
	4	22.124	15.782	18.720	11.113	18.447	7.7819	1.439	4.377	−3.229	4.104
	5	14.382	14.135	11.675	4.466	16.799	3.1869	2.939	0.479	−6.729	5.603

Table 2 Comparison of several small target detection algorithms for Fig. 2.

	LSBR					*LSBRG*				
	M-Med	M-Mean	TDLMS	FKT	PPCA	M-Med	M-Mean	TDLMS	FKT	PPCA
Fig. 2(a)	13.673	3.896	12.036	4.518	26.302	1.294	−8.483	−0.344	−7.862	13.922
Fig. 2(d)	9.212	2.408	9.385	3.767	20.202	0.062	−6.742	0.235	−5.383	11.052
Fig. 2(g)	16.038	12.413	6.255	9.684	18.400	7.881	4.255	−1.902	1.527	10.242
Fig. 2(j)	9.382	7.782	7.365	11.285	17.789	0.170	−1.430	−1.848	2.073	8.577
	5.344	7.495	2.726	1.146	9.547	0.386	2.537	−2.233	−3.812	4.589
Fig. 2(m)	14.572	11.570	10.143	9.804	31.133	0.506	−2.495	−3.923	−4.261	17.068
Fig. 2(p)	7.587	6.717	3.040	5.698	16.589	−3.315	−4.184	−7.862	−5.203	5.687

local region, therefore we define *local signal to background ratio* (*LSBR*) as the signal to background ratio in a window around the region of interest. The *LSBR* (in *dB*) is defined as the following:

$$LSBR = 10\log_{10}\frac{\sum_{i=L_x}^{H_x}\sum_{j=L_y}^{H_y}(I(i,j)-m_b)^2}{\sigma_b^2} \tag{14}$$

where (L_x, L_y) and (H_x, H_y) define the window of interest, i.e. the window that contains the targets, $I(i, j)$ is the intensity of the pixels within this window, m_b and ${\sigma_b}^2$ are the mean value and the variance of the background around the target respectively. Also we define the *LSBR gain* (*LSBRG*) as the following(in *dB*), which is another significant judge of the effectiveness of a detection algorithm:

$$LSBRG = LSBRG_{out} - LSBRG_{in} \tag{15}$$

where $LSBR_{out}$ and $LSBR_{in}$ are the *LSBR* of a target region after and before the detection respectively. A larger *LSBRG* means after detection *LSBR* has been significantly raised which indicates a better algorithm performance.

Tables 1 and 2 show the *LSBR* and *LSBRG* of target regions in Figs. 1 and 2 after detection, using different detection algorithms. It can be seen obviously from these tables that among all the algorithms used in the experiments PPCA gives the largest *LSBR* and *LSBRG*, which means that the proposed algorithm gives the best performance and is most effective.

5 Conclusions

In this paper, a new infrared small target detection method is proposed using probabilistic PCA (PPCA), which is an extension of PCA and reformulated PCA in a probabilistic framework. Just like using PCA for face detection known as the "eigenface" method, we take a similar approach using PPCA for small target detection, by first computing the weight matrix in the subspace using training samples created using Gaussian intensity function, and then compare the distance between the original image vector and the reconstructed image vector. Experiments have shown the effectiveness of the proposed algorithm.

References

1. M. E. Tipping and C. M. Bishop, "Probabilistic principle component analysis," Journal of Royal Statistical Society, Series B **61** (Part 3), 611–622 (1999).
2. M. E. Tipping and C. M. Bishop, "Mixtures of probabilistic principal component analysers," Neural Computation **11** (2), 443–482, MIT Press (1999).
3. C. M. Bishop, "Variational principal component analysis," Proceedings Ninth International Conference on Artificial Neural Networks, ICANN'99, IEE, Vol. 1, pp. 509–514.
4. G. Boccignone, A. Chianese, and A. Picariello, "Small target detection using wavelets," Proceedings of IEEE 4th International Conference on Pattern Recognition **8**, 1776–1778 (1998).
5. F. A. Sadjadi, "IR target detection using probability density functions of wavelet transform subbands," Applied Optics, The Optical Society of America Publication **43** (2), 315–323 (2004).
6. H. Kwon and N. Nasrabadi, "Kernel spectral matched filter for hyperspectral imagery," International Journal of Computer Vision **71** (2), 127–141 (2007).

7. H. Leung and A. Young, "Small target detection in clutter using recursive nonlinear prediction," IEEE Transactions on Aerospace and Electronic Systems **36** (2), 713–718 (April 2000).
8. L. Chan, S. Z. Der, and N. M. Nasrabadi, "A joint compression-discrimination neural transformation applied to target detection," IEEE Transactions on Systems, Man, and Cybernetics, Part B, 670–681 (2005).
9. M. Turk and A. Pentland, "Eigenface for recognition," Journal of Cognitive Neural Science **3** (1), 71–86 (1991).
10. M.-H. Yang, D. J. Kriegman, and N. Ahuja, "Detecting faces in images: a survey," IEEE Transactions on Pattern Analysis and Machine Intelligence **24** (1), 34–58 (2002).
11. A. Mahalanobis, R. R. Muise, S. R. Stanfill, and A. Van Nevel, "Design and application of quadratic correlation filters for target detection," IEEE Transactions on Aerospace and Electronic Systems **40** (3), 837–850 (2004).
12. Z. Liu, C. Chen, X. Shen, and X. Zou, "Detection of small objects in image data based on the nonlinear principal component analysis neural network," Optical Engineering **44** (9), 093604 (2005).
13. C. M. Dwan and S. Z. Der, "A neural network based target detection system for FLIR imagery," Proceedings of SPIE **3307**, 14–21 (1998).
14. S. D. Deshpande, M. H. Er, R. Venkateswarlu, and P. Chan, "Max-mean and max-median filters for detection of small targets," Proceedings of SPIE **3809**, 74–83 (1999).
15. T. Soni, R. Zeidler, and W. H. Ku,"Performance of 2-D adaptive prediction filters for detection of small objects in image data," IEEE Transactions on Image Processing **2** (3), 327–340 (1993).